Trace elements in $PM_{2.5}$ shed light over Saharan dust incursions over Munich airshed in spring 2022

S. Padoan[1], A. Zappi[2], Jan Bendl[1], T. Herrmann[1], A. P. Mudan[1], Carsten Neukirchen[1], Erika Brattich[3], Laura Tositti[2], T. Adam[1]

[1] University of the Bundeswehr Munich, Faculty for Mechanical Engineering, Institute of Chemical and Environmental Engineering, Werner-Heisenberg-Weg 39, 85577, Neubiberg, Germany

[2]University of Bologna, Department of Chemistry "G. Ciamician", Bologna, Italy

[3] University of Bologna, Department of Physics and Astronomy "Augusto Righi", Bologna, Italy

Corresponding author: Sara Padoan (sara.padoan@unibw.de)

Supplementary material

Table S1. Signal-to-noise ratio (SNR), background equivalent concentrations (BEC), limits of detection (LoD) and limits of quantification (LoQ) for all the elements. All data are in µg L^{-1}.

Element	SNR	BEC	LOD	LOQ
Na	1	77.6	79	82
Mg	0.7	1.18	2	3
Al	0.6	2.16	3	4
Ca	5	21.2	26	38
S	0.3	3.35	4	4
K	4	29.6	34	44
Cr	0.013	0.0920	0.10	0.13
Mn	0.03	0.0339	0.06	0.13
Fe	0.07	1.25	1.3	1.5
Co	0.0010	0.00481	0.006	0.008
Ni	0.03	0.108	0.14	0.2
Cu	0.011	0.119	0.13	0.2
Zn	0.2	3.19	3	4
V	0.002	0.00213	0.004	0.009
As	0.005	0.0121	0.02	0.03
Sr	0.017	0.119	0.14	0.2
Se	0.02	0.00838	0.03	0.09
Mo	0.006	0.0150	0.02	0.03
Cd	0.002	0.00319	0.006	0.011
Sb	0.002	0.00497	0.007	0.011
Ba	0.007	0.192	0.2	0.2
Pb	0.015	0.0919	0.11	0.14

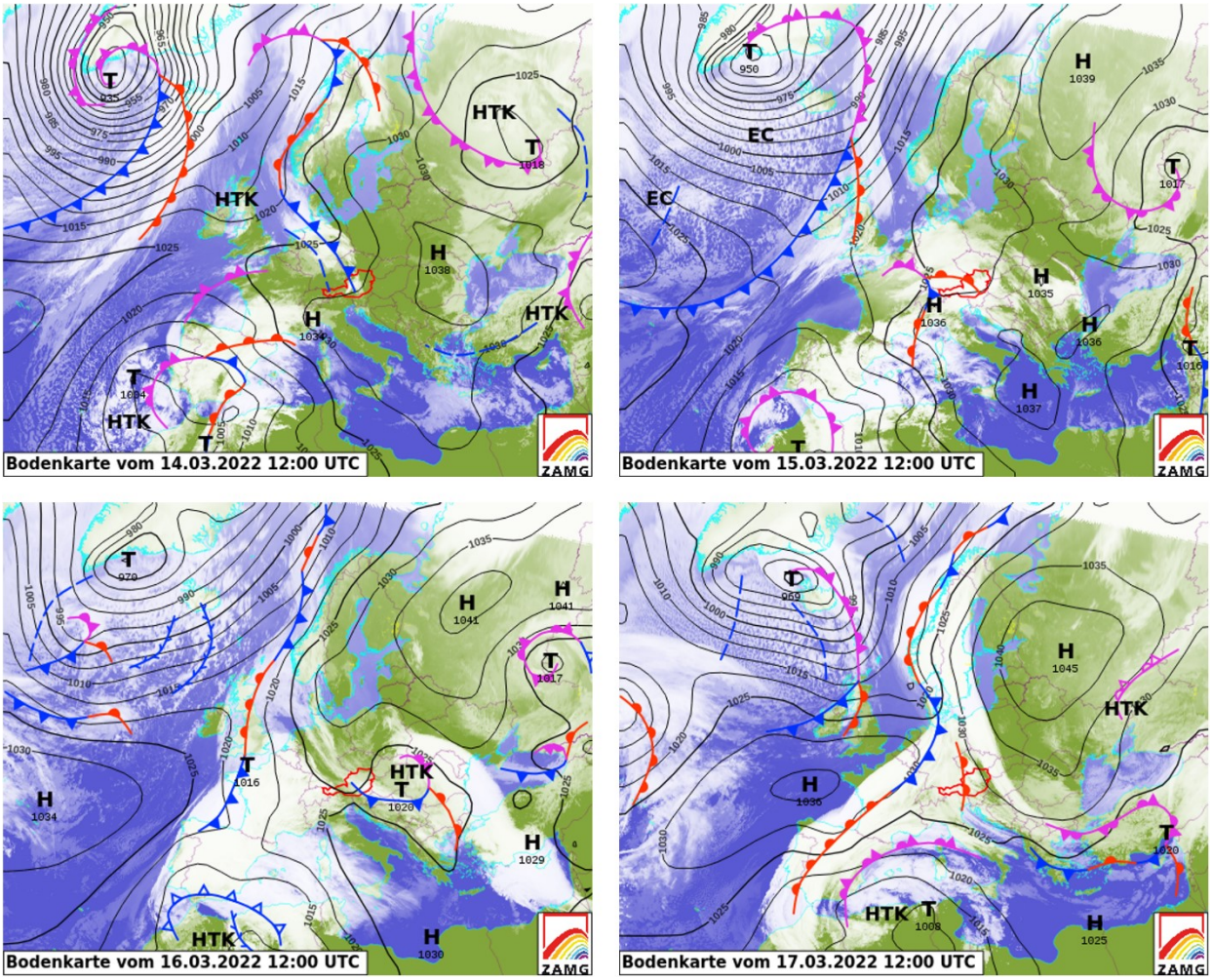

Figure S1. Synoptic situation for the period of 14-17 March 2022 (from top-left to bottom-right). 'H' and 'T' indicate, respectively, the centers of high and low pressure systems). Source: Zentralanstalt für Meteorologie und Geodynamik (ZAMG), Austria.

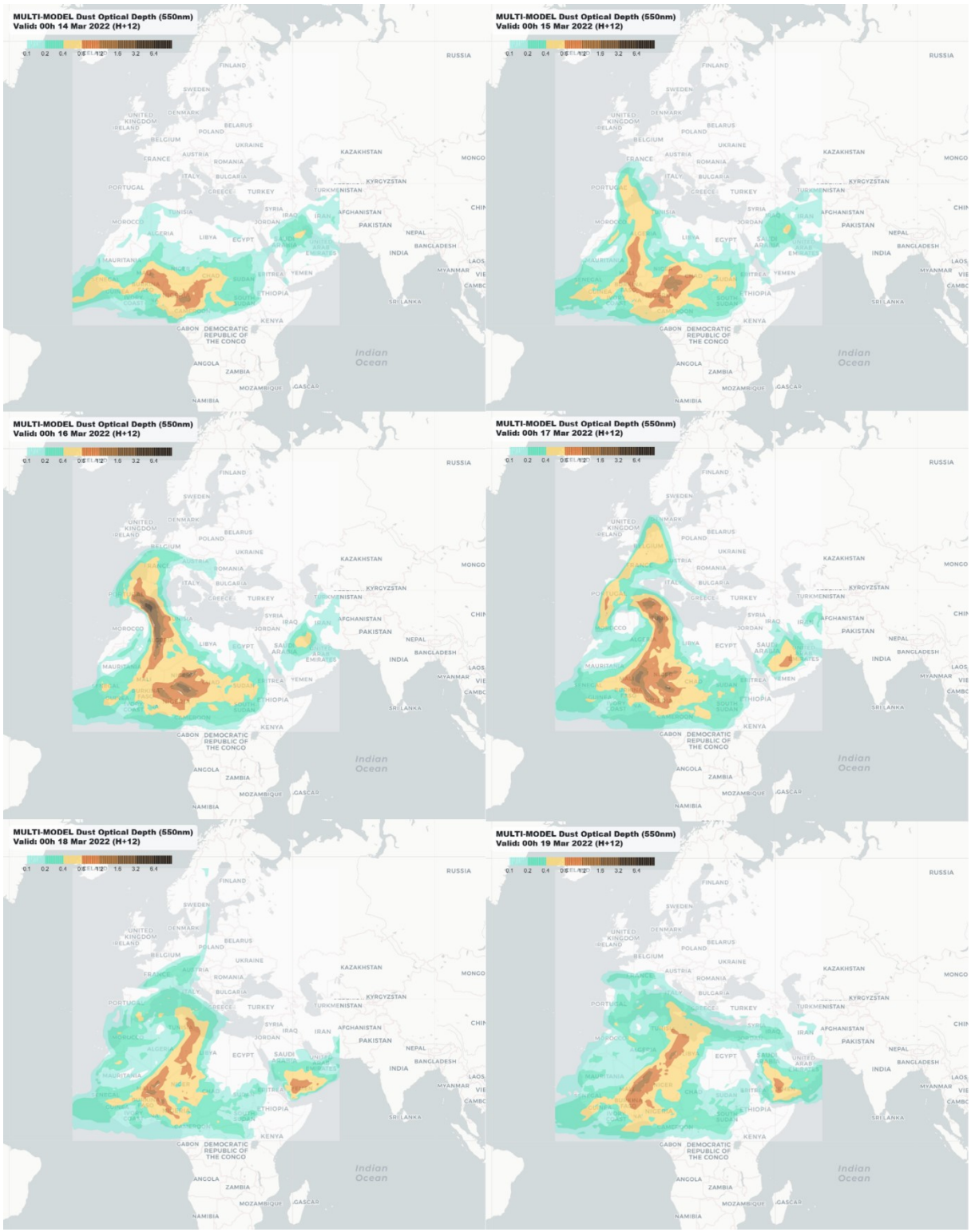

Figure S2. Multimodel forecast of dust optical depth at 550 nm, for the period 14-19 March 2022 (from top-left to bottom-right), 12 UTC. Source: SDS-WAS from AEMET and the Barcelona Dust Center.

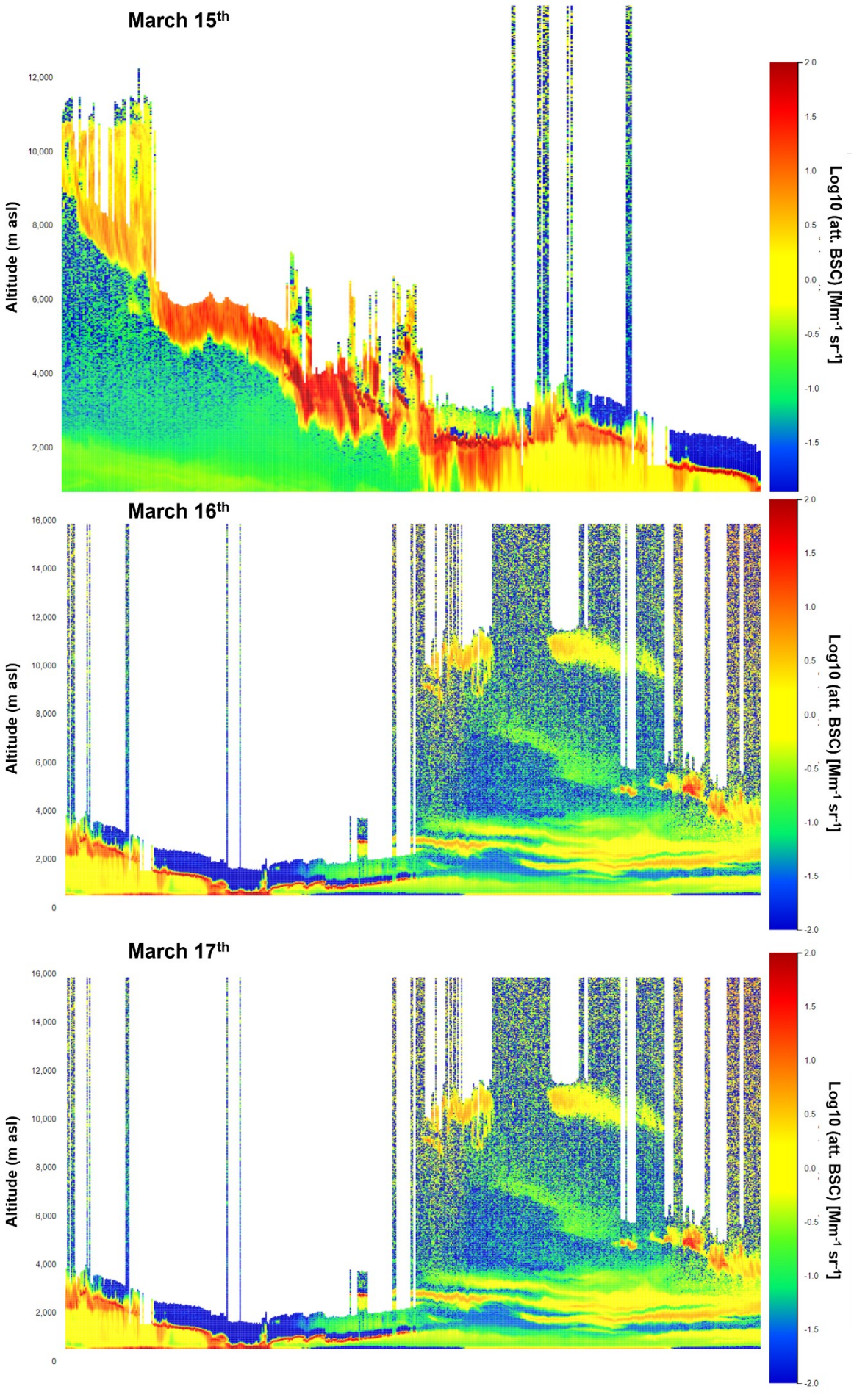
March 15th
March 16th
March 17th
Altitude (m asl)
Log10 (att. BSC) [Mm-1 sr-1]
12,000
10,000
8,000
6,000
4,000
2,000
16,000
14,000
0
2.0
1.5
1.0
0.5
0.0
-0.5
-1.0
-1.5
-2.0

Figure S3. Time-series of the vertical profiles of attenuated backscatter coefficient measured at a ceilometer network, coordinated by E-PROFILE of the EUMETNET Composite Observing System, EUCOS (https://e-profile.eu/) at Oberschleissheim nearby Munich for 15-16-17March 2022.

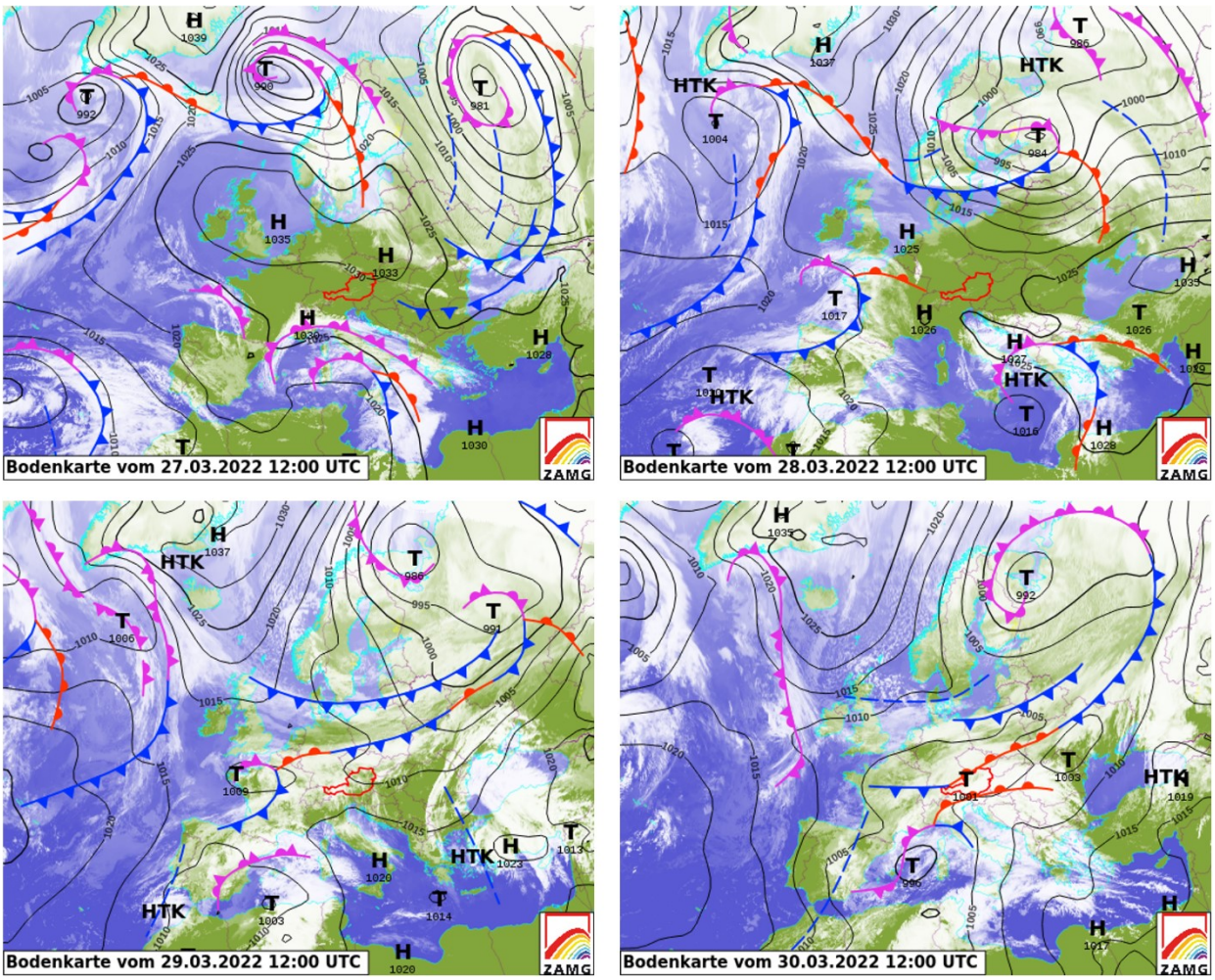

Figure S4. Synoptic situation for the period of 27-30 March 2022 (from top-left to bottom-right). 'H' and 'T' indicate, respectively, the centers of high and low pressure systems. Source: Zentralanstalt für Meteorologie und Geodynamik (ZAMG), Austria.

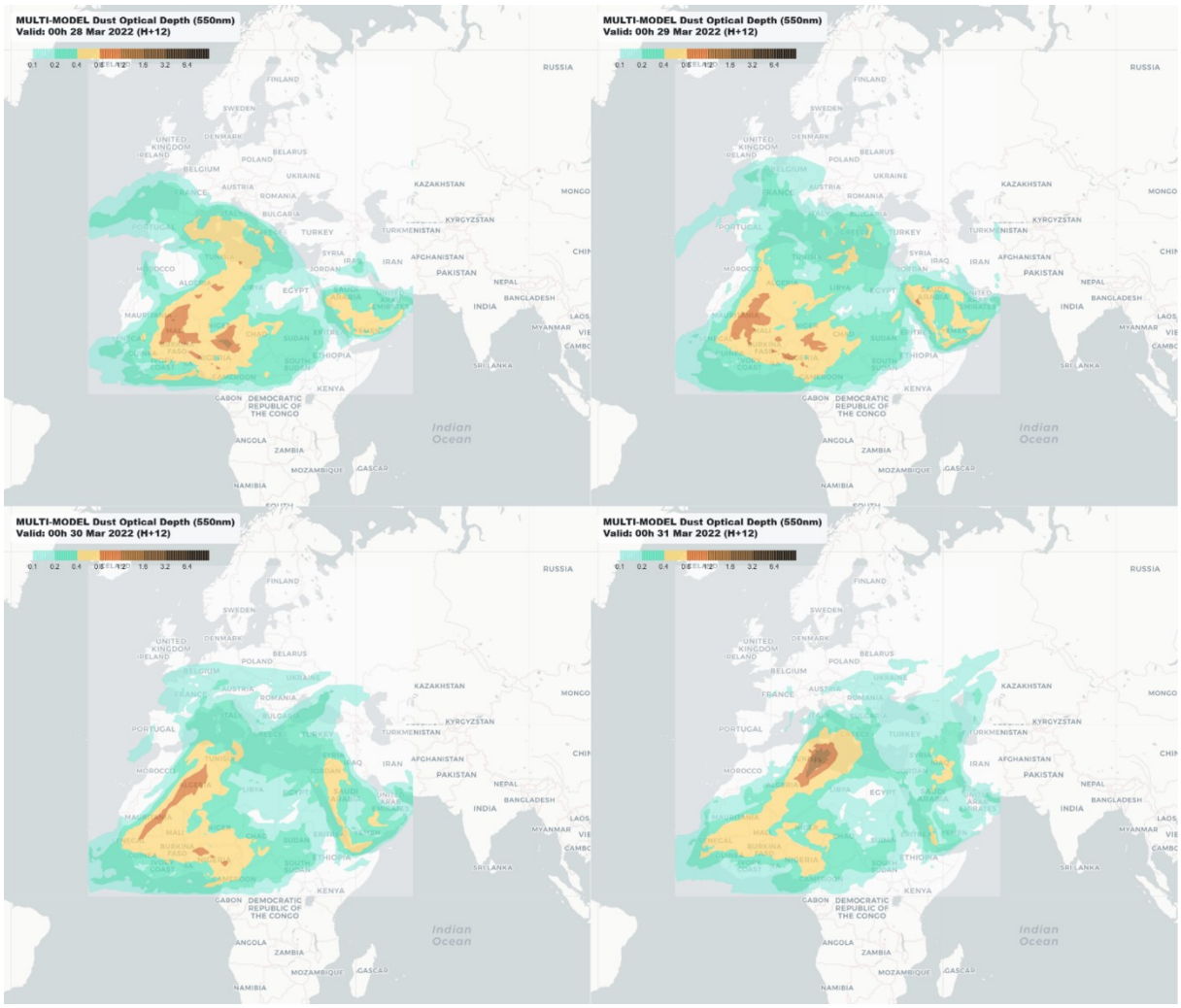

Figure S5. Multimodel forecast of dust optical depth at 550 nm, for the period 28-31 March 2022 (from top-left to bottom-right), 12 UTC. Source: SDS-WAS from AEMET and the Barcelona Dust Center.

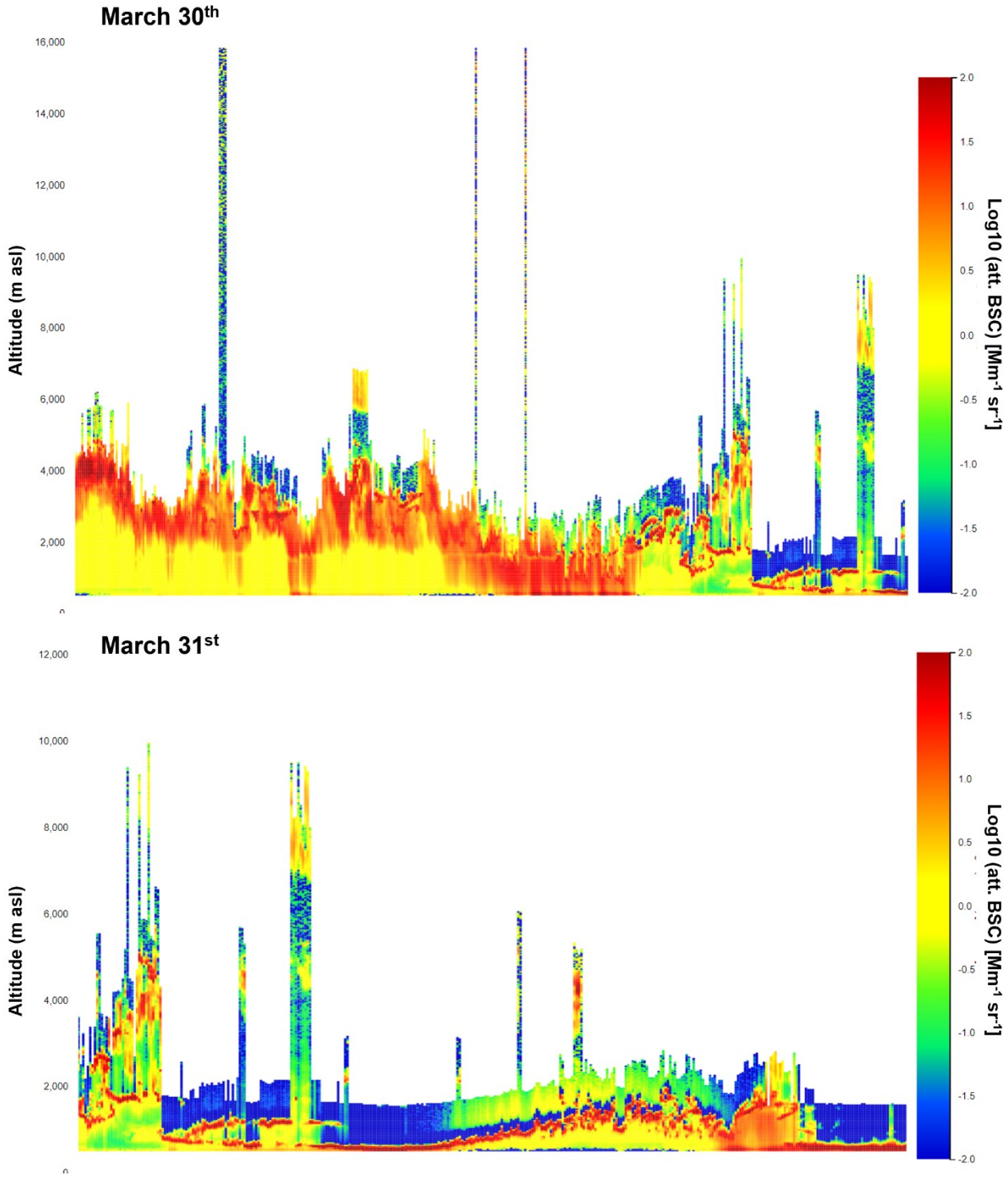

Figure S6. Time-series of the vertical profiles of attenuated backscatter coefficient measured at a ceilometer network, coordinated by E-PROFILE of the EUMETNET Composite Observing System, EUCOS (https://e-profile.eu/) at Oberschleissheim nearby Munich for 30-31 March 2022.

Table S2. Varimax loadings for metal concentrations in the reduced-dataset case, without SD-affected days. Bold values correspond to the most representative variables for each factor, EV stands for the explained variance.

	Factor 1	**Factor 2**	**Factor 3**	**Factor 4**	**Factor 5**	**Factor 6**
EV (%)	19.8	18.89	14.71	9.65	8.81	5.1
Na	-0.24	-0.24	-0.15	0.18	0.05	-0.20
Mg	-0.06	**-0.41**	-0.07	-0.09	0.08	-0.10
Al	0.03	-0.25	0.05	-0.28	-0.13	-0.35
Ca	0.07	**-0.46**	0.12	-0.19	-0.07	0.11
S	**0.45**	0.12	0.05	-0.18	0.06	-0.01
K	0.16	0.05	0.08	**0.44**	-0.09	-0.01
Cr	-0.03	0.02	**-0.55**	-0.11	-0.03	0.15
Mn	-0.01	0.14	**-0.52**	-0.03	-0.06	0.14
Fe	0.14	-0.23	-0.26	0.07	-0.06	-0.09
Co	0.00	-0.06	-0.10	-0.02	0.23	**0.73**
Ni	0.08	-0.21	0.07	**-0.51**	-0.05	0.18
Cu	0.11	-0.15	**-0.28**	0.04	-0.08	-0.22
Zn	-0.12	-0.01	0.00	0.05	**-0.61**	0.08
V	0.04	0.01	-0.02	0.02	**-0.62**	0.18
As	**0.32**	0.02	0.12	0.07	-0.33	0.08
Sr	0.03	**-0.45**	0.15	0.08	0.04	0.22
Se	**0.45**	0.08	0.03	0.03	0.13	-0.07
Mo	0.00	-0.12	**-0.34**	0.12	0.03	-0.05
Cd	**0.38**	-0.09	-0.08	0.10	-0.02	0.09
Sb	0.20	-0.22	-0.16	0.16	0.01	-0.12
Ba	-0.02	-0.25	0.14	**0.53**	0.06	0.16
Pb	**0.40**	0.01	-0.09	0.02	0.08	-0.04

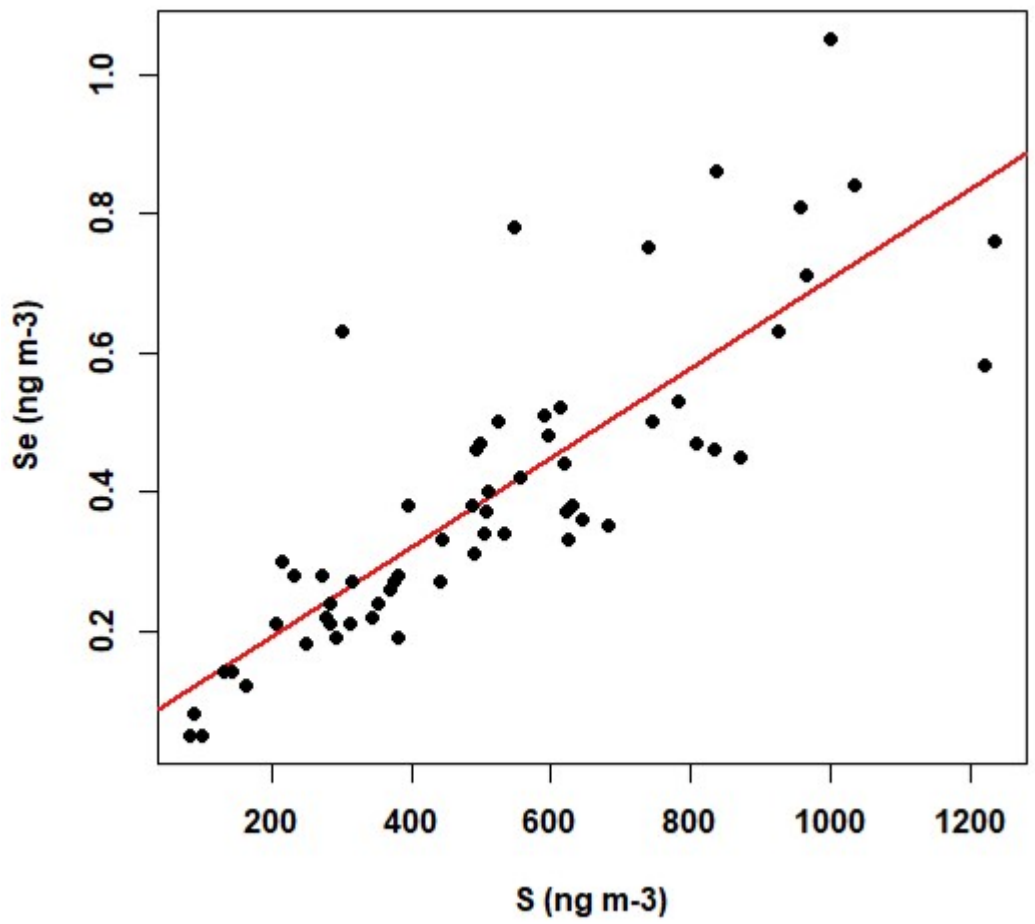

Figure S7. Linear relation between Se and S

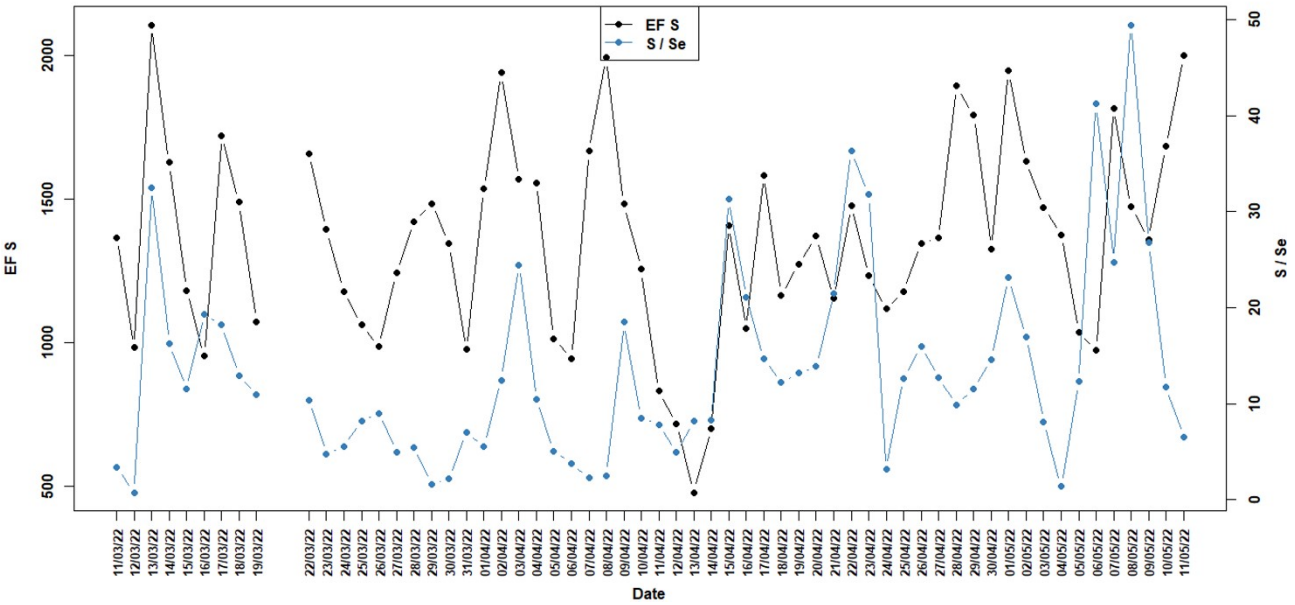

Figure S8. Comparison of the time trends of sulfur EF and the ratio S/Se.